

Maximum Entangled State in Ultracold Spin-1 Mixture

Jie Zhang,^{1,*} Longsheng Yu,¹ Zezhen He,¹ and Pengjun Wang^{2,†}

¹*College of Physics, Taiyuan University of Technology,
Taiyuan 030024, Shanxi, People's Republic of China*

²*State Key Laboratory of Quantum Optics and Quantum Optics Devices,
Institute of Opto-electronics, Shanxi University Taiyuan Shanxi 030006, People's Republic of China*

Inspired by the method that can deterministically generate the massive entanglement through phase transitions, we study the ground state properties of a spin-1 condensate mixture, under the premise that the heteronuclear spin-exchange collision is taken into account. We developed an effective model to analyze the binary-coupled two-level system and studied the ground state phase transitions. Three representative quantum states with the same number distribution are studied and distinguished through the number fluctuations. We demonstrate that there will be the Greenberger-Horne-Zeilinger (GHZ) state in the mixture if the extra magnetic field is specifically selected or adiabatically adjusted. One advantage of preparing entangled states in mixtures is that we only need to adjust the external magnetic field, instead of considering the microwaves-magnetic cooperation. Finally we estimate the feasibility of experimentally generating the heteronuclear many-body entanglement in the alkali-metal atomic mixture.

PACS numbers: 03.75.Mn, 67.60.Bc, 67.85.Fg

I. INTRODUCTION

Quantum entanglement [1] is a fundamental yet intriguing quantum phenomenon, the coherence and non-locality make it distinguished from classical physics. Besides the essence of quantum mechanics, the generated entanglement states are important resources for applications in many fields, including quantum information [2], quantum computation [3, 4] quantum metrology [5, 6] and quantum cryptography [7]. How to generate stable entangled states has become a hot topic in fundamental science frontier recent years.

Greenberger-Horne-Zeilinger (GHZ) state is one of the ultimate goals for quantum information and quantum metrology, due to its extraordinary precision guaranteed by fundamental quantum principles. However, it is challenging to create entanglement states in multi-particle ensembles, although efforts have been made at different platforms [8–13], including 20-qubits GHZ state in Rydberg atom arrays [14] and superconducting quantum circuit [15]. The required precision of the control and technical difficulties making it difficult to increase the size of the entanglement states. Recently, GHZ states are created in optical cavity, by shifting the energy of a particular Dicke state to convert unentangled states into entangled states [16], where 100-atom GHZ state can be obtained with a fidelity at 0.92, and the one with 2000 atoms can be achieved with a fidelity at 0.89.

The spin-exchanging collisions [17–22] inside Bose-Einstein condensates (BEC) is also one of the popular candidates to produce multiparticle entanglement state, such as spin squeezed states [23–25], spin-nematic squeez-

ing states [26], Dicke states [27–29], and twin-Fock states [30–32]. Recent years, the condensate mixtures and heteronuclear spin-exchanging collisions have also attracted a lot of attentions [33–42]. A unique feature of the spin-1 mixture is that the inter-species spin-spin interaction takes place over all three total spin $F=0,1$, and 2 channels. Besides this, the Zeeman energy shift of hyperfine states for different atoms are quite different in the same magnetic field, which make it possible to select special spin-exchange channels.

In this paper, we theoretically analyse the possibility to generate the multi-particle GHZ states in the mixture of spin-1 condensates, on the premise of adjusting the external magnetic field adiabatically. The assumption of adiabatically adjust magnetic field has been realized in the single spin-1 condensate, where more than 1000-atom entangled twin-Fock condensate was generated deterministically [32]. The advantage of preparing entangled states in mixtures is that we only need to adjust the external magnetic field, instead of considering the microwaves-magnetic cooperation. Moreover, we propose near-deterministic generation, instead of dynamical. The latter can also lead to fluctuations and degradation of the entanglement.

The outline of this paper is as follows: Sec. II introduces the model hamiltonian, the spin-exchange processes, the Zeeman effects, and the reduced spin-exchange process in the extra fields. In Sec. III, we give an effective reduced hamiltonian to analytically explain the special ground states and calculate the observables, such as number fluctuation and number distribution, as well as the quantities that can characterize and measure entanglement. In Sec. IV, we discuss possible parameter ranges to capture or realize the entanglement state experimentally. Conclusions are made at the end in Sec. V.

*Electronic address: zhangjie01@tyut.edu.cn

†Electronic address: Pengjun.wang@sxu.edu.cn

II. THE MODEL HAMILTONIAN

In the spinor mixture, the angular momentum coupling between heteronuclear atoms do not obey the identity principle any more, which cause the heteronuclear spin interaction between spin-1 atoms takes place over all three total spin $F=0,1$, and 2 channels. The *inter-species* spin-exchange interaction can be expressed as,

$$V_{12}(\mathbf{r}) = \frac{1}{2}(\alpha + \beta \mathbf{f}_1 \cdot \mathbf{f}_2 + \gamma P_0)\delta(\mathbf{r}), \quad (1)$$

where the parameters $\alpha = (g_1 + g_2)/2$, $\beta = (g_1 - g_2)/2$, and $\gamma = (2g_0 + g_2 - 3g_1)/2$, are the linear combinations of the coupling constants $g_F = \frac{2\pi\hbar^2 a_F}{\mu}$. a_F are *s*-wave scattering lengths in the total spin $F=0,1,2$ channels. $\mu = \frac{\mu_1\mu_2}{\mu_1+\mu_2}$ denotes the reduced mass for atoms in different species and \hbar is the Planck's constant. P_0 projects an inter-species pair into spin singlet state only through the $F=0$ channel.

Including the *intra-species* spin-exchange interaction, the spin-dependent Hamiltonian for the mixture under the single-mode approximation (SMA) [19, 20] finally takes the form $H = H_1 + H_2 + H_{12}$, where

$$H_1 = c_1\beta_1 \frac{\mathbf{L}_1^2}{N_1} + p_1(\hat{n}_1 - \hat{n}_{-1}) + q_1(\hat{n}_1 + \hat{n}_{-1}), \quad (2)$$

$$H_2 = c_2\beta_2 \frac{\mathbf{L}_2^2}{N_2} + p_2(\hat{n}'_1 - \hat{n}'_{-1}) + q_2(\hat{n}'_1 + \hat{n}'_{-1}), \quad (3)$$

$$H_{12} = c_{12}\beta \frac{\mathbf{L}_1 \cdot \mathbf{L}_2}{N_{12}} + c_{12}\gamma \frac{\Theta_{12}^\dagger \Theta_{12}}{N_{12}}. \quad (4)$$

The number operators for two species are defined as

$$\hat{n}_0 = \hat{a}_0^\dagger \hat{a}_0, \hat{n}_{\pm 1} = \hat{a}_{\pm 1}^\dagger \hat{a}_{\pm 1}, \quad (5)$$

$$\hat{n}'_0 = \hat{b}_0^\dagger \hat{b}_0, \hat{n}'_{\pm 1} = \hat{b}_{\pm 1}^\dagger \hat{b}_{\pm 1}, \quad (6)$$

and $p_{1,2}(q_{1,2})$ denotes the linear (quadratic) Zeeman field energy for the two species. Parameter $\beta_{1,2} = 4\pi\hbar^2 a_{1,2}/\mu_{1,2}$ denotes the intra-species spin-exchange interaction, and the sign of which determines the polar (+) or ferromagnetic (-) feature of a spinor condensate respectively. c_1 , c_2 and c_{12} are tunable parameters determined by particle numbers and trapping frequencies. $\mathbf{L}_1 = a_{m_1}^\dagger(\mathbf{f}_1)_{m_1 n_1} a_{n_1}$ and $\mathbf{L}_2 = b_{m_2}^\dagger(\mathbf{f}_2)_{m_2 n_2} b_{n_2}$ are the spin-1 angular momentum operator for the two species, operator Θ_{12}^\dagger creates a singlet pair with one atom each from the two species. More comprehensive and detailed presentations given by $a_{m_1}(b_{m_2})$ and $a_{m_1}^\dagger(b_{m_2}^\dagger)$ are presented in the appendix A.

III. GROUND STATE PROPERTIES

To study the effects of the interspecies spin-exchange interaction, one would like to suppress the intraspecies parts. This can be done by choosing suitable parameters

$q_{1,2}$. A microwave [30] can also contribute to the parameter $q_{1,2}$, so that the linear and the quadratic Zeeman field can actually be controlled independently. Consider the situation that linear Zeeman field is comparable to the quadratic Zeeman field, the case $p_1 = -q_1$ can suppress the \hat{n}_1 population of the first species. Similarly, if $p_2 = q_2$, the population on the \hat{n}'_{-1} of the second species are suppressed. In this paper we mainly focus on the process-4 (see appendix A) which has the advantage to discuss the heteronuclear spin-exchange physics in the subspace with the total magnetization equals to zero.

A. Effective Hamiltonian and basis

In the chosen and fixed extra fields, the total Hamiltonian (4) reduces to a more simple and symmetric case with only four Zeeman components involved:

$$H_{12} = -[\Gamma_1 + \Gamma_2](\hat{n}_{-1}\hat{n}'_1 + \hat{n}_0\hat{n}'_0) - \Gamma_2\hat{n}_{-1}\hat{n}'_1 + \Gamma_1(\hat{a}_{-1}^\dagger \hat{b}_1^\dagger \hat{b}_0 \hat{a}_0 + \hat{a}_0^\dagger \hat{b}_0^\dagger \hat{a}_{-1} \hat{b}_1), \quad (7)$$

where

$$\Gamma_1 = c_{12}(g_1 - g_0), \Gamma_2 = c_{12} \frac{g_2 - g_1}{2}. \quad (8)$$

If g_2 is independently tunable, we can achieve a special point with $\Gamma_2 = 0$, which make the Hamiltonian (7) more symmetric and analyzable. This is a binary-coupled two-level system, each species can be consider as a two-level quantum oscillator. Similar to the two-site Bose-Hubbard model, terms like $\hat{a}_{-1}^\dagger \hat{b}_1^\dagger \hat{b}_0 \hat{a}_0$ can denote the "hopping-like" interactions, while the term $\hat{n}_{-1}\hat{n}'_1$ or $\hat{n}_{-1}\hat{n}'_1$ represents the density-interaction between particles. The Hilbert space can be expanded by the Fock states that describe the particle-occupation on four different energy levels $|n_{-1}, n_0\rangle \otimes |n'_0, n'_1\rangle$, or alternatively, we can rewrite them as $|m_1\rangle \otimes |m_2\rangle$, with $m_1 = n_{-1} - n_0$, and $m_2 = n'_0 - n'_1$. If we consider the special case of $N_1 = N_2 = N$ and for even N , we can rewrite the basis as:

$$|m_1\rangle \otimes |m_2\rangle = |M, m\rangle, \quad (9)$$

where we define $M = m_1 + m_2$ and $m = m_1 - m_2$. Still further, the unique properties of process-4 (vanishing the total spin) guarantees that $M = 0$, and only one parameter m is needed to describe the different basis:

$$|n_{-1}, n_0, n'_0, n'_1\rangle \equiv |m\rangle. \quad (10)$$

The ground state is a superposition states of all basis, $|G\rangle = \sum_m \Psi_m |m\rangle$.

B. Different phases

For analysis purposes, we first consider a hypothetical Hamiltonian which is more symmetrical and analyzable:

$$H = \Gamma_1(\hat{A}^\dagger \hat{B} + \hat{B}^\dagger \hat{A}) - (\Gamma_1 + \Gamma_2)(\hat{n}_{-1}\hat{n}'_1 + \hat{n}_0\hat{n}'_0). \quad (11)$$

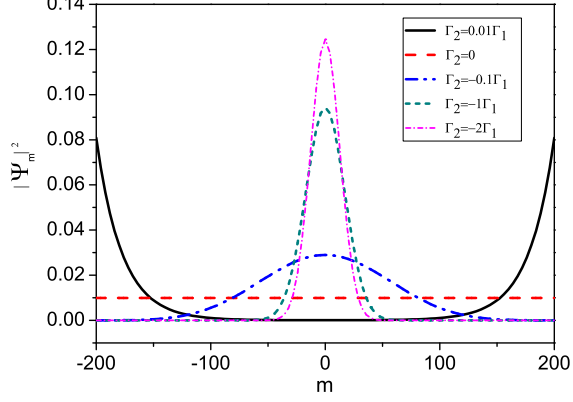


FIG. 1: (Color online) The ground state amplitude distribution $|\Psi_m|^2$ of spin-1 mixture in a fixed magnetic field. The values of m represent different basis, and the parameter Γ_2 is assumed to be adjustable. The total numbers are $N_1 = N_2 = 100$.

The parameter Γ_2 is adjustable which can range from positive to negative. Without loss of generality, we first consider the positive parameter Γ_1 and fixed it to be one. $\hat{A}^\dagger = \hat{a}_0^\dagger \hat{b}_0^\dagger$, and $\hat{B}^\dagger = \hat{a}_{-1}^\dagger \hat{b}_1^\dagger$ are the pair creation operators for each species. Minimizing the energy (11), one can get the profile $|\Psi_m|^2$ for different phases. The numerical results are demonstrated in Fig.1, where the total particle numbers are $N_1 = N_2 = 100$. It's obviously that the special point with $\Gamma_2 = 0$ are the critical point.

1. special states when $\Gamma_2 < 0$

When $\Gamma_2 < 0$, the ground state profile $|\Psi_m|^2$ presents a Gaussian distribution. In this region, the special point with $\Gamma_2 = -\Gamma_1$ is particularly comprehensible, that means there are no density interactions between particles and the hopping process $\hat{A}^\dagger \hat{B} + \hat{B}^\dagger \hat{A}$ dominates the system. The ground state is a direct product of two independent coherent states,

$$\begin{aligned} |G\rangle_c &= \frac{(\hat{a}_0^\dagger + \hat{a}_{-1}^\dagger)^N |0\rangle}{\sqrt{2^N N!}} \otimes \frac{(\hat{b}_1^\dagger + \hat{b}_0^\dagger)^N |0\rangle}{\sqrt{2^N N!}} \\ &= \frac{1}{2^N N!} (\hat{a}_0^\dagger \hat{b}_1^\dagger + \hat{a}_0^\dagger \hat{b}_0^\dagger + \hat{a}_{-1}^\dagger \hat{b}_1^\dagger + \hat{a}_{-1}^\dagger \hat{b}_0^\dagger)^N |0\rangle. \end{aligned} \quad (12)$$

The average numbers of atoms in the four components are exactly all equal to $N/2$, the number fluctuations on this point is exactly

$$\Delta n_{-1} = \Delta n_0 = \Delta n'_0 = \Delta n'_1 = \sum_m m^2 \Psi_m^2. \quad (13)$$

When $\Gamma_2 < -\Gamma_1$, the coherence of product state still maintain, but can be shifted as Γ_2 is adjusted. The

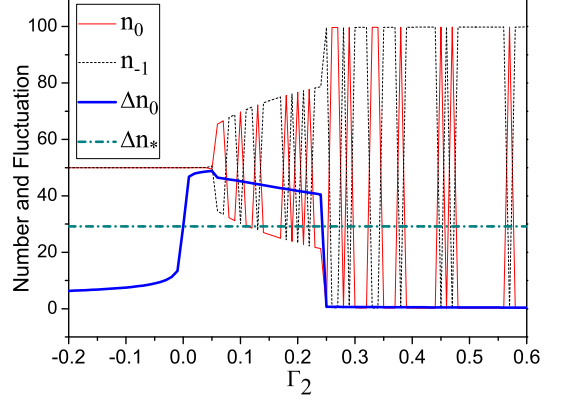


FIG. 2: (Color online) The Zeeman-level number distributions n_0 (red solid) and n_{-1} (black dashed), the number fluctuation Δn_0 (blue solid) of the species A are presented, as the interaction parameter Γ_2 is adjustable and in the unit of Γ_1 . The total numbers are $N_1 = N_2 = 100$. The black dashed line (Δn_*) which denote the 0-component number fluctuation of the special ground state $|G\rangle_*$ is also displayed for comparison. The Zeeman-level number distributions and fluctuations of the species B which are either strictly equal to or opposite to the presentations, are not shown.

decreasing of Γ_2 can suppress particle fluctuations between different components and narrow the Gaussian toward the delta-function [43], which corresponds to a Fock state,

$$|m=0\rangle = \left| \frac{N}{2}, \frac{N}{2}, \frac{N}{2}, \frac{N}{2} \right\rangle. \quad (14)$$

In the region $-\Gamma_1 < \Gamma_2 < 0$, as demonstrated in Fig.1, the Gaussian distribution is broadened as Γ_2 is increasing, until the distribution is totally flat on the point $\Gamma_2 = 0$.

When $\Gamma_2 = 0$, this point gives us a uniform distribution state with $|\Psi_m|^2 = \frac{1}{N+1}$, or, $|G\rangle_* = \sum_m \frac{1}{\sqrt{N+1}} |m\rangle$. Equivalently, we can prove that this state has an analytical form:

$$|G\rangle_* = \frac{1}{2^N N!} (\hat{a}_0^\dagger \hat{b}_0^\dagger + \hat{a}_{-1}^\dagger \hat{b}_1^\dagger)^N |0\rangle. \quad (15)$$

The number fluctuations on this point is exactly,

$$\Delta n_{0,-1} = \Delta n'_{0,1} = \sqrt{\frac{N(2N+1)}{6} - \frac{N^2}{4}}. \quad (16)$$

2. special state when $\Gamma_2 > 0$

When $\Gamma_2 > 0$, the ground state split into a bimodal distribution state, which indicates a Schrodinger Cat like state (CAT-state) [43]: $|G\rangle_{cat} = \frac{1}{\sqrt{2}} (|m_L\rangle + |m_R\rangle)$,

$$|m_L\rangle = |m = -2N\rangle = |N, 0, 0, N\rangle, \quad (17)$$

$$|m_R\rangle = |m = +2N\rangle = |0, N, N, 0\rangle, \quad (18)$$

or simply denoted as,

$$|G\rangle_{cat} = \frac{1}{\sqrt{2}}(|-1\rangle_1^{\otimes N} |1\rangle_2^{\otimes N} + |0\rangle_1^{\otimes N} |0\rangle_2^{\otimes N}), \quad (19)$$

which is illustrated by a two-body Newton's pendulum in Fig.3.

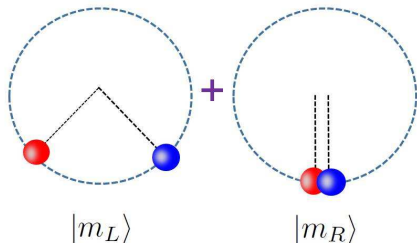


FIG. 3: (Color online) Two-particle Newton's pendulum can demonstrate the characteristics of the maximum entanglement state in spin-1 BEC mixture. Red balls denote the particles from A system, and blue balls denote the particles from B system. Two balls on the equilibrium position can be regarded as the dead-cat state or $|m_R\rangle$, while two balls on the highest position is the live-cat state or $|m_L\rangle$.

The splitting from Gaussian distribution to CAT-state distribution is in fact a spontaneous symmetry breaking process. The latter is extremely unstable and can exist only when Γ_2 is slightly greater than 0. The comparable strength between "hopping" and "interaction" can lead to the CAT-state, otherwise, the system has to chosen one possible state at a time between two Fock states $|m_L\rangle$ and $|m_R\rangle$. We calculate the particle numbers and number fluctuations on CAT-state and find that the average numbers of atoms in the four components are exactly all equal to $N/2$, while the number fluctuations are macroscopical ($\sim N$), which indicate that this is a fragmented BEC mixture [44].

It is difficult to distinguish $|G\rangle_*$ from $|G\rangle_{cat}$ by the number distributions ($n_{0,-1} = n'_{0,1} = N/2$), however, the number fluctuations can reveal the secret and distinct different phases, see Fig.2. When $\Gamma_2 < 0$, the fluctuation is small and flat, then the fluctuation of particle number increases significantly near $\Gamma_2=0$, that means system enter the state $|G\rangle_*$. In the region $0 < \Gamma_2 < \frac{1}{4}$ where Γ_2 is tinely greater than 0, we notice that the number fluctuations of state $|G\rangle_{cat}$ is higher that the number fluctuations of the state $|G\rangle_*$. Moreover, two number states are populated simultaneously in this region, that means there are multi-particle GHZ states in the spinor mixture.

When $\Gamma_2 > \frac{1}{4}$, the number fluctuation drop dramatically and the number distribution of n_0 is capricious between 0 and 100 as Γ_2 is adjusted. This reflects the fact that there is a trivial Fock state after the spontaneous symmetry breaking, however, which number state to populate is totally random.

C. The GHZ state and entanglement entropy

The GHZ state is a certain type of entangled state that involves at least three qubits, and its most remarkable characteristics can be demonstrated intuitively by the density matrix. For example, one maximally entangled state of tripartite, $\Phi = \frac{1}{\sqrt{2}}(|000\rangle + |111\rangle)$, its density operator is

$$\rho = \frac{1}{2} \begin{bmatrix} 1 & 0 & 0 & 0 & 0 & 0 & 0 & 1 \\ 0 & 0 & 0 & 0 & 0 & 0 & 0 & 0 \\ 0 & 0 & 0 & 0 & 0 & 0 & 0 & 0 \\ 0 & 0 & 0 & 0 & 0 & 0 & 0 & 0 \\ 0 & 0 & 0 & 0 & 0 & 0 & 0 & 0 \\ 0 & 0 & 0 & 0 & 0 & 0 & 0 & 0 \\ 0 & 0 & 0 & 0 & 0 & 0 & 0 & 0 \\ 1 & 0 & 0 & 0 & 0 & 0 & 0 & 1 \end{bmatrix},$$

which is a square matrix with non-zero elements in the four corners and zero elements elsewhere. The GHZ state in our Fock state basis can be described as $\Phi_{GHZ} = \frac{1}{\sqrt{2}}(|m_L\rangle + |m_R\rangle)$, and its density operator is

$$\rho = \frac{1}{2} \begin{bmatrix} 1 & 0 & \dots & 0 & 1 \\ 0 & \dots & \dots & \dots & 0 \\ \vdots & \dots & \dots & \dots & \vdots \\ \vdots & \dots & \dots & \dots & \vdots \\ 0 & \dots & \dots & \dots & 0 \\ 1 & 0 & \dots & 0 & 1 \end{bmatrix},$$

with the dimension of matrix equals to the numbers of basis (9).

For the bipartite quantum system, the measure of entanglement can be given by the partial von Neumann entropy. The von Neumann entropy of a state is defined as

$$S(\rho) = -Tr(\rho \log \rho), \quad (20)$$

where the symbol ρ is the density operator for the system and $Tr(\dots)$ denotes the trace operation. For the bipartite A-B system, the degree of entanglement can be defined as the von Neumann entropy of reduced density operators ρ_A or ρ_B , which is defined as ,

$$\rho_A = -Tr_B[\rho_{AB}], \rho_B = -Tr_A[\rho_{AB}], \quad (21)$$

where ρ_{AB} is the density operator of the whole system. We can diagonalize ρ_A (or ρ_B) so that the partial von Neumann entropy for the entanglement degree can be written as

$$S(\rho_A) = - \sum_n (\rho_n \log \rho_n), \quad (22)$$

where the symbols ρ_n are the non-negative eigenvalues of the reduced density operator ρ_A , and sum to unity, $\sum \rho_n = 1$.

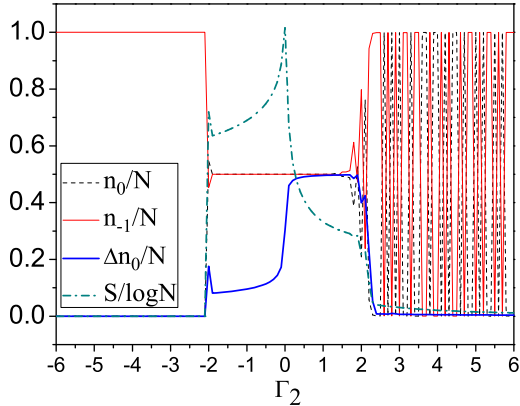


FIG. 4: (Color online) The Zeeman-level number distributions n_0 (black dashed) and n_{-1} (red solid), the number fluctuation Δn_0 (blue solid), and the partial von Neumann entropy S (green dash-dot) of special A are presented, as the interaction parameter Γ_2 is adjustable and in the unit of Γ_1 . The number distributions and fluctuations of particles in special B which are either strictly equal to or opposite to the presentations are not shown. The total numbers are $N_1 = N_2 = 20$.

In order to understand the properties more comprehensively, we consider the full-space expansion with the basis $|m_1\rangle \otimes |m_2\rangle$, and $N = N_1 = N_2 = 20$. We diagonalize the Hamiltonian (7) and track the entanglement characteristic using the partial von Neumann entropy $S(\rho_A)$, which is illustrated in different interacting regions, see Fig.(4). We found that there is a zone with no-zero entropy (no-matter $\Gamma_2 < 0$ or $\Gamma_2 > 0$), which is always associated with the equally distributed particles on the four Zeeman-level:

$$n_{-1} = n_0 = n'_0 = n'_1 = N/2. \quad (23)$$

In the $\Gamma_2 < 0$ region, the degree of entanglement is higher and keep growing until $\Gamma_2 = 0$. On the $\Gamma_2 = 0$ point, the top value $S(\rho_A)=1$, confirms the knowledge that the uniform distribution state $|G\rangle_*$ is the maximally entangled State.

So far, we have discussed the entanglement properties of the coherent state, the uniform distribution state, and the CAT-state. Since particles are indistinguishable in BECs and it is not possible to determine which particles occupy a particular spatial pattern, one should explore other possible ways to divide the system. In consideration of the fact that how many particles occupy a spatial pattern can be measured physically, the subspace A or B can be divided according to two distinguishable spatial patterns. In our case, we divided the system by the two spatially incompatible BECs, and each BEC contains two models respectively. Even if there are 40 particles in the system, the system's entanglement is still based on only four modes. In this perspective, the maximum entangled state of the four-mode BEC-mixture should be the

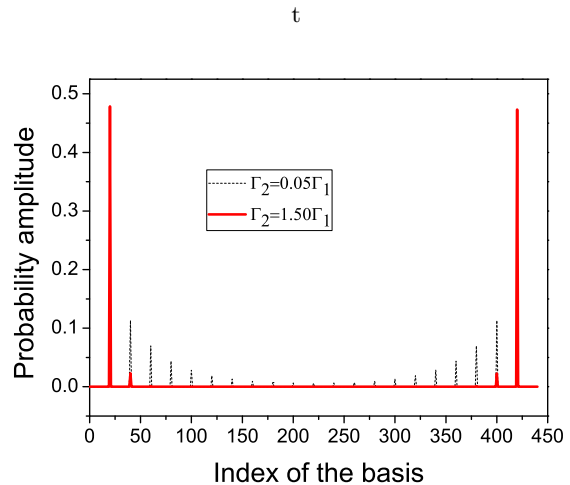


FIG. 5: (Color online) The ground state amplitude distribution $|\Psi_{M,m}|^2$ of spin-1 mixture. The horizontal axis displays the index of basis and the ordinate value is the amplitude. We pick up two representative points, $\Gamma_2 = 0.05\Gamma_1$ and $\Gamma_2 = 1.5\Gamma_1$, to illustrate the basic properties. The total particle number is $N_1 = N_2 = 20$ and the total number of basis is 441.

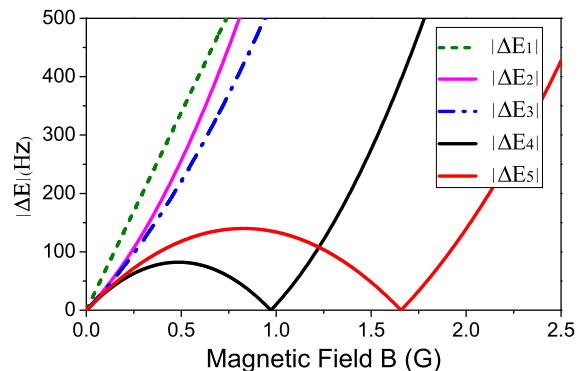


FIG. 6: (Color online) The dependence of heteronuclear magnetic energy differences on the applied magnetic field. Two processes represented by ΔE_4 and ΔE_5 have zero-crossing points at $B = 0.97G$ and $B = 1.69G$ respectively, while other processes show large detuning. The energy differences ΔE_i can be both positive and negative, here we took their absolute values to make the picture more compact.

uniform distribution state $|G\rangle_*$. The well-known GHZ or Cat state, on the contrary, present the lower entanglement degree. In Fig.(5), we illustrated the ground state profile $|\Psi_{M,m}|^2$ s for two representative points in region $\Gamma_2 > 0$, and the red line confirms the Schroedinger's Cat properties: simultaneous occupation on two opposite states, large fluctuations and no zero entanglement entropy.

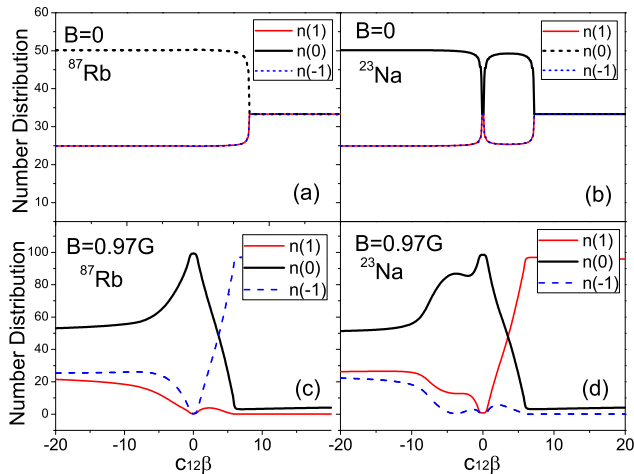


FIG. 7: (Color online) Numerical calculation of Zeeman level number distributions of Na-Rb mixture in a fixed magnetic field $B_0 = 0$ and $B_0 = 0.97G$. The intraspecies interactions of Na species are fixed to be $c_1\beta_1 = 1$, and other interacting parameters are in the unit of $c_1\beta_1$. The intraspecies interactions of Rb species is set to be $c_2\beta_2 = -2$ without loss of generality. The interspecies interaction $c_{12}\beta$ is assumed to be adjustable and can range from negative to positive. parameter γ is much smaller than β and has been neglected.

IV. PARAMETER ESTIMATION AND EXPERIMENTAL REALIZATION

In this section, we discuss the possibility of realizing the inter-species entanglement state in the ultra-cold Na^{23} and Rb^{87} mixture. The Zeeman shifts $E_{m_1}^{(1)}$ and $E_{m_2}^{(2)}$ can be calculated by the Breit-Rabi formula, which can give the corresponding Zeeman energy differences ΔE_i (before and after scattering) for the 5 processes:

$$\begin{aligned}\Delta E_1 &= E_0^{(1)} + E_{-1}^{(2)} - E_{-1}^{(1)} - E_0^{(2)}, \\ \Delta E_2 &= E_0^{(1)} + E_1^{(2)} - E_1^{(1)} - E_0^{(2)}, \\ \Delta E_3 &= E_0^{(1)} + E_0^{(2)} - E_{-1}^{(1)} - E_1^{(2)}, \\ \Delta E_4 &= E_0^{(1)} + E_0^{(2)} - E_1^{(1)} - E_{-1}^{(2)}, \\ \Delta E_5 &= E_{-1}^{(1)} + E_1^{(2)} - E_1^{(1)} - E_{-1}^{(2)}.\end{aligned}$$

By appropriately applying the Zeeman field [40], people can select out one special spin-exchange process, with the related Zeeman energy differences ΔE_i vanished. The other spin-exchange channels are forbidden, because the corresponding Zeeman energy differences show large detunings, see Fig.(6).

In Fig.(7), we shows the dependence of the number distributions on the inter-species interaction $c_{12}\beta$ at two fixed values of magnetic field. The numerical results are obtained through the approach of exact diagonalizing the total Hamiltonian $H = H_1 + H_2 + H_{12}$, and H_{12} is the original Hamiltonian (A6). The basis we considered is

the direct product of spin-1 Fock states:

$$\left|n_1^{(1)}, n_0^{(1)}, n_{-1}^{(1)}\right\rangle \otimes \left|n_1^{(2)}, n_0^{(2)}, n_{-1}^{(2)}\right\rangle, \quad (24)$$

but, the total magnetization is limited with $m_{tot} = m_1 + m_2 = 0$.

When the magnetic field is absent, there are FF phase (or coherent state) when $c_{12}\beta \ll -1$, and the AA phase when $c_{12}\beta \gg 1$ [35], the later is a fragmented state with particle number equally distributed in three Zeeman levels. The $c_{12}\beta = 0$ point means independent, which shows the characteristic particle number distribution $(N/4, N/2, N/4)$ and $(N/3, N/3, N/3)$ for Rb^{87} and Na^{23} respectively.

On the point $c_{12}\beta = 0$ and $B=0.97G$, particles only distribute on the $n_0^{(1)}$ and $n_0^{(2)}$ components respectively, that is the typical quadratic Zeeman effect [32, 45, 46] for spin-1 BEC.

When the inter-species spin-exchange interaction is not zero, and $c_{12}\beta > 0$. The remarkable properties for the spin-exchange effects are highlighted, as illustrated in Fig.2(c) and Fig.2(d). The selected process-4 will finally drive the the ground state number distributions from $(0, N, 0)$ to $(0, 0, N)$ for Rb BEC, and from $(0, N, 0)$ to $(N, 0, 0)$ for Na BEC. We notice that there is a crossover point, where the numbers are equally distributed on four Zeeman-levels. That means the interacting region near the crossover point can possibly contain the three distinctive states that we have discussed before.

The background s-wave scattering lengths of Na^{23} and Rb^{87} heteronuclear interaction have been calculated in [39]. They are $a_0=82.71a_B$, $a_1=81.4a_B$, and $a_2=78.9a_B$, which results in the reality that

$$\Gamma_1 = \frac{2\pi\hbar^2 a_B}{\mu}(-1.31), \Gamma_2 = \frac{2\pi\hbar^2 a_B}{\mu}(-2.5), \quad (25)$$

and we have $\Gamma_2:\Gamma_1 \approx 1.9$. The ground state amplitude distribution calculated under the above parameters, is quite similar to the result illustrated in Fig.(5), and the partial von Neumann entropy is about $S(\rho_A)=0.29924$.

V. CONCLUSION

To conclude, we study the quantum ground states of the spin-1 mixture, where two adjacently prepared ultra-cold atomic gases can mapping to the double-well model, and still further, there are two hyperfine states in each well. Firstly, we studied three distinctive ground states, they are the mixed coherent state $|G\rangle_c$, the uniform distribution state $|G\rangle_*$, and the CAT-state $|G\rangle_{cat}$. We distinguished them through number fluctuations on different Zeeman-levels, and gave a analytical expression of state $|G\rangle_*$. Furthermore, we calculated the partial von Neumann entropy in different interacting region, and found that both $|G\rangle_c$ and $|G\rangle_{cat}$ had non zero entanglement entropy. The von Neumann entropy for $|G\rangle_*$ is exactly equals to 1, which indicated that this is a maximum

mixed state. The ground state amplitude distribution for $|G\rangle_c$ is gaussian, for $|G\rangle_{cat}$, it is bimodal. The state $|G\rangle_*$, however, has a exactly uniform ground state amplitude distribution.

Since particles are indistinguishable in BECs, we have to divide the system by the spatially incompatible pattern, so called mode-division. In our case, two BECs next to each other is a natural two-mode structure, more than that, two hyperfine states inside each BECs finally lead to four independent modes. In this perspective, the maximum entangled state of the four-mode BEC-mixture is the $|G\rangle_*$, with entropy $S(\rho_A)=1$. The well-known GHZ state or maximum entanglement state of qubits, on the contrary, present the lower entanglement degree. The existence of the GHZ state is confirmed through the ground state amplitude distribution and the density matrix directly. Additionally, our GHZ state is not strictly meet the traditional definition, because there are four internal

spin states involved simultaneously, this can be described by a Schrodinger cat like Newton-pendulum.

Finally, we consider the experimental realization. The Zeeman shifts $E_{m_1}^{(1)}$ and $E_{m_2}^{(2)}$ at the intensity about 0.97G can lead to the binary-coupled two-level spin-exchange model, no additional necessary of applying the microwave. According to the calculation of the $\text{Na}^{23}\text{-Rb}^{87}$ background s-wave scattering lengths, the interaction coincidentally located in the Cat-state region. We assume that adiabatically adjusting the magnetic field can drive the mixture into a Heteronuclear GHZ state. Our results highlight the significant promises for experimental generation of GHZ state in atomic condensate simply through adjusting the magnetic field.

This work is supported by the Natural Science Foundation of Shanxi Province (Grant No. 202103021224051)

-
- [1] R. Horodecki, P. Horodecki, M. Horodecki, and K. Horodecki, Quantum entanglement, *Rev. Mod. Phys.* **81**, 865 (2009).
- [2] O. Gühne and G. Tóth, Entanglement detection, *Phys. Rep.* **474**, 1 (2009).
- [3] K. Kim, M.-S. Chang, S. Korenblit, R. Islam, E. Edwards, J. Freericks, G.-D. Lin, L.-M. Duan, and C. Monroe, Quantum simulation of frustrated Ising spins with trapped ions, *Nature (London)* **465**, 590 (2010).
- [4] J. Simon, W. S. Bakr, R. Ma, M. E. Tai, P. M. Preiss, and M. Greiner, Quantum simulation of antiferromagnetic spin chains in an optical lattice, *Nature (London)* **472**, 307 (2011).
- [5] V. Giovannetti, S. Lloyd, and L. Maccone, Advances in quantum metrology, *Nat. Photonics* **5**, 222 (2011).
- [6] H. Aasi et al., Enhanced sensitivity of the LIGO gravitational wave detector by using squeezed states of light, *Nat. Photonics* **7**, 613 (2013).
- [7] M. A. Taylor, J. Janousek, V. Daria, J. Knittel, B. Hage, H.-A. Bachor, and W. P. Bowen, Subdiffraction-Limited Quantum Imaging within a Living Cell, *Phys. Rev. X* **4**, 011017 (2014).
- [8] M. J. Holland and K. Burnett, Interferometric detection of optical phase shifts at the Heisenberg limit, *Phys. Rev. Lett.* **71**, 1355 (1993).
- [9] A. S. Sorensen and K. Molmer, Entanglement and Extreme Spin Squeezing, *Phys. Rev. Lett.* **86**, 4431 (2001).
- [10] K. S. Choi, A. Goban, S. B. Papp, S. J. van Enk, and H. J. Kimble, Entanglement of spin waves among four quantum memories, *Nature (London)* **468**, 412 (2010).
- [11] C. Gross, H. Strobel, E. Nicklas, T. Zibold, N. Bargill, G. Kurizki and M. K. Oberthaler, Atomic homodyne detection of continuous-variable entangled twin-atom states, *Nature* **480**, 219 (2011).
- [12] B. Lüke, M. Scherer, J. Kruse, L. Pezzé, F. Deuretzbacher, P. Hyllus, O. Topic, J. Peise, W. Ertmer, J. Arlt, L. Santos, A. Smerzi, C. Klempt, Twin Matter Waves for Interferometry Beyond the Classical Limit, *Science* **334**, 773 (2011).
- [13] Z. Zhang and L.-M. Duan, Generation of Massive Entanglement through an Adiabatic Quantum Phase Transition in a Spinor Condensate, *Phys. Rev. Lett.* **111**, 180401 (2013).
- [14] A. Omran, H. Levine, A. Keesling, G. Semeghini, T. T. Wang, S. Ebadi, H. Bernien, A. S. Zibrov, H. Pichler, S. Choi, J. Cui, M. Rossignolo, P. Rembold, S. Montangero, T. Calarco, M. Endres, M. Greiner, V. Vuletic, and M. D. Lukin, Generation and manipulation of Schrodinger cat states in Rydberg atom arrays, *Science* **365**, 570 (2019).
- [15] C. Song, K. Xu, H. Li, Y.-R. Zhang, X. Zhang, W. Liu, Q. Guo, Z. Wang, W. Ren, J. Hao, H. Feng, H. Fan, D. Zheng, D.-W. Wang, H. Wang, and S.-Y. Zhu, Generation of multicomponent atomic Schrodinger cat states of up to 20 qubits, *Science* **365**, 574 (2019).
- [16] Zhao, Y., Zhang, R., Chen, W. et al. Creation of Greenberger-Horne-Zeilinger states with thousands of atoms by entanglement amplification. *npj Quantum Inf* **7**, 24 (2021).
- [17] T.-L. Ho, Spinor Bose Condensates in Optical Traps, *Phys. Rev. Lett.* **81**, 742 (1998).
- [18] T. Ohmi and K. Machida, Bose-Einstein Condensation with Internal Degrees of Freedom in Alkali Atom Gases, *J. Phys. Soc. Jpn.* **67**, 1822 (1998).
- [19] C. K. Law, H. Pu, and N. P. Bigelow, Quantum Spins Mixing in Spinor Bose-Einstein Condensates, *Phys. Rev. Lett.* **81**, 5257 (1998).
- [20] S. Yi, Ö. E. Müstecaplioglu, C. P. Sun, and L. You, Single-mode approximation in a spinor-1 atomic condensate, *Phys. Rev. A* **66**, 011601(R) (2002).
- [21] M.-S. Chang, Q. S. Qin, W. X. Zhang, L. You, and M. S. Chapman, Coherent spinor dynamics in a spin-1 Bose condensate, *Nat. Phys.* **1**, 111 (2005).
- [22] D. M. Stamper-Kurn and M. Ueda, Spinor Bose gases: Symmetries, magnetism, and quantum dynamics, *Rev. Mod. Phys.* **85**, 1191 (2013).
- [23] A. Sørensen, L.-M. Duan, J. I. Cirac, and P. Zoller, Many-particle entanglement with Bose-Einstein condensates, *Nature (London)* **409**, 63 (2001).
- [24] C. Gross, T. Zibold, E. Nicklas, J. Estève, and M. K. Oberthaler, Atomic homodyne detection of continuous-

- variable entangled twin-atom states, *Nature (London)* 464, 1165 (2010).
- [25] M.F. Riedel, P. Böhi, Y. Li, T.W. Hänsch, A. Sinatra, and P. Treutlein, Atom-chip-based generation of entanglement for quantum metrology, *Nature (London)* 464, 1170 (2010).
- [26] C.D.Hamley, C. S. Gerving, T. M. Hoang, E. M. Bookjans, and M. S. Chapman, Spin-nematic squeezed vacuum in a quantum gas, *Nat. Phys.* 8, 305 (2012).
- [27] K. S. Choi, A. Goban, S. B. Papp, S. J. van Enk, and H. J. Kimble, *Nature (London)* 468, 412 (2010).
- [28] C. Gross, H. Strobel, E. Nicklas, T. Zibold, N. Bargill, G. Kurizki and M. K. Oberthaler, *Nature* 480, 219 (2011).
- [29] B. Lücke, M. Scherer, J. Kruse, L. Pezzé, F. Deuretzbacher, P. Hyllus, O. Topic, J. Peise, W. Ertmer, J. Arlt, L. Santos, A. Smerzi, C. Klempt, *Science* 334, 773 (2011).
- [30] M. J. Holland and K. Burnett, *Phys. Rev. Lett.* 71, 1355 (1993).
- [31] A. S. Sorensen and K. Molmer, Entanglement and Extreme Spin Squeezing, *Phys. Rev. Lett.* 86, 4431 (2001).
- [32] Xin-Yu Luo, Yi-Quan Zou, Ling-Na Wu, Qi Liu, Ming-Fei Han, Meng Khoon Tey, and Li You, Deterministic entanglement generation from driving through quantum phase transitions, *Science* 355, 620-623 (2017).
- [33] M. Luo, Z. Li, and C. Bao, Bose-Einstein condensate of a mixture of two species of spin-1 atoms, *Phys. Rev. A* 75, 043609 (2007).
- [34] Zhi-fang Xu, Jie Zhang, Yunbo Zhang, and Li You, Quantum states of a binary mixture of spinor Bose-Einstein condensates, *Phys. Rev. A* 81, 033603 (2010).
- [35] Jie Zhang, Zhi-Fang Xu, Li You, and Yunbo Zhang, Atomic-number fluctuations in a mixture of condensates, *Phys. Rev. A* 82, 013625 (2010).
- [36] Jie Zhang, Tiantian Li, and Yunbo Zhang, Interspecies singlet pairing in a mixture of two spin-1 Bose condensates, *Phys. Rev. A* 83, 023614 (2011).
- [37] Yu Shi, Ground states of a mixture of two species of spinor Bose gases with interspecies spin exchange, *Phys. Rev. A* 82, 023603 (2010).
- [38] Jie Zhang, Xue Hou, Bin Chen, and Yunbo Zhang, Fragmentation of a spin-1 mixture in a magnetic field, *Phys. Rev. A* 91, 013628 (2015).
- [39] F. D.Wang, D. Z. Xiong, X. K. Li, D. J.Wang, and E. Tiemann, Observation of Feshbach resonances between ultracold Na and Rb atoms, *Phys. Rev. A* 87, 050702(R) (2013).
- [40] Xiaoke Li, Bing Zhu, Xiaodong He, Fudong Wang, Mingyang Guo, Zhi-Fang Xu, Shizhong Zhang, and Dajun Wang, Coherent Heteronuclear Spin Dynamics in an Ultracold Spinor Mixture, *Phys. Rev. Lett.* 114, 255301 (2015).
- [41] A. Burchianti, C. D'Errico, S. Rosi, A. Simoni, M. Modugno, C. Fort and F. Minardi, Dual-species Bose-Einstein condensate of 41K and 87Rb in a hybrid trap, *Phys. Rev. A* 98, 063616 (2018).
- [42] C. D'Errico, A. Burchianti, M. Prevedelli, L. Salasnich, F. Ancilotto, M. Modugno, F. Minardi, and C. Fort, *Phys. Rev. Research* 1, 033155 (2019).
- [43] T.-L. Ho and C. V. Ciobanu, The Schrodinger Cat Family in Attractive Bose Gases and Their Interference, arXiv.0011095v1 (2000).
- [44] T.-L. Ho and S.-K. Yip, Fragmented and Single Condensate Ground States of Spin-1 Bose Gas, *Phys. Rev. Lett.* 84, 4031 (2000).
- [45] J. Stenger, S. Inouye, D. M. Stamper-Kurn, H.-J. Miesner, A. P. Chikkatur and W. Ketterle, Spin domains in ground-state Bose-Einstein condensates, *Nature (London)* 396, 345 (1998).
- [46] L.E. Sadler, J. M. Higbie, S. R. Leslie, M. Vengalattore, and D. M. Stamper-Kurn, Spontaneous symmetry breaking in a quenched ferromagnetic spinor Bose-Einstein condensate, *Nature (London)* 443, 312 (2006).

Appendix A: The full Hamiltonian and basis

We take the first species for example, where $\mathbf{L}_1 = \hat{a}_{m_1}^\dagger(\mathbf{f}_1)_{m_1 n_1} \hat{a}_{n_1}$ are defined in terms of 3×3 spin-1 matrices $f_x, f_y,$ and f_z , discussions for the other species can just replace the operator $\hat{a}_{m_1}^\dagger(\hat{a}_{n_1})$ with $\hat{b}_{m_1}^\dagger(\hat{b}_{n_1})$:

$$\begin{aligned} L_x &= \frac{1}{\sqrt{2}} \begin{pmatrix} \hat{a}_1^\dagger & \hat{a}_0^\dagger & \hat{a}_{-1}^\dagger \end{pmatrix} \begin{pmatrix} 0 & 1 & 0 \\ 1 & 0 & 1 \\ 0 & 1 & 0 \end{pmatrix} \begin{pmatrix} \hat{a}_1 \\ \hat{a}_0 \\ \hat{a}_{-1} \end{pmatrix} \\ &= \frac{1}{\sqrt{2}} (\hat{a}_1^\dagger \hat{a}_0 + \hat{a}_0^\dagger \hat{a}_1 + \hat{a}_0^\dagger \hat{a}_{-1} + \hat{a}_{-1}^\dagger \hat{a}_0) \end{aligned} \quad (\text{A1})$$

$$\begin{aligned} L_y &= \frac{i}{\sqrt{2}} \begin{pmatrix} \hat{a}_1^\dagger & \hat{a}_0^\dagger & \hat{a}_{-1}^\dagger \end{pmatrix} \begin{pmatrix} 0 & -i & 0 \\ i & 0 & -i \\ 0 & i & 0 \end{pmatrix} \begin{pmatrix} \hat{a}_1 \\ \hat{a}_0 \\ \hat{a}_{-1} \end{pmatrix} \\ &= \frac{-i}{\sqrt{2}} (\hat{a}_1^\dagger \hat{a}_0 + \hat{a}_0^\dagger \hat{a}_{-1} - \hat{a}_0^\dagger \hat{a}_1 - \hat{a}_{-1}^\dagger \hat{a}_0) \end{aligned} \quad (\text{A2})$$

$$\begin{aligned} L_z &= \begin{pmatrix} \hat{a}_1^\dagger & \hat{a}_0^\dagger & \hat{a}_{-1}^\dagger \end{pmatrix} \begin{pmatrix} 1 & 0 & 0 \\ 0 & 0 & 0 \\ 0 & 0 & -1 \end{pmatrix} \begin{pmatrix} \hat{a}_1 \\ \hat{a}_0 \\ \hat{a}_{-1} \end{pmatrix} \\ &= \hat{a}_1^\dagger \hat{a}_1 - \hat{a}_{-1}^\dagger \hat{a}_{-1} \end{aligned} \quad (\text{A3})$$

The Hamiltonians represented by the creation and annihilation operator are:

$$\begin{aligned} H_1 &= \beta_1 [\hat{n}_1(\hat{n}_1 - 1) + \hat{n}_{-1}(\hat{n}_{-1} - 1)] \\ &\quad + \beta_1 [-2\hat{n}_1\hat{n}_{-1} + 2\hat{n}_1\hat{n}_0 + 2\hat{n}_0\hat{n}_{-1}] \\ &\quad + \beta_1 (\hat{a}_1^\dagger \hat{a}_{-1}^\dagger \hat{a}_0 \hat{a}_0 + \hat{a}_0^\dagger \hat{a}_0^\dagger \hat{a}_1 \hat{a}_{-1}), \end{aligned} \quad (\text{A4})$$

$$\begin{aligned} H_2 &= \beta_2 [\hat{n}'_1(\hat{n}'_1 - 1) + \hat{n}'_{-1}(\hat{n}'_{-1} - 1)] \\ &\quad + \beta_2 [-2\hat{n}'_1\hat{n}'_{-1} + 2\hat{n}'_1\hat{n}'_0 + 2\hat{n}'_0\hat{n}'_{-1}] \\ &\quad + \beta_2 (\hat{b}_1^\dagger \hat{b}_{-1}^\dagger \hat{b}_0 \hat{b}_0 + \hat{b}_0^\dagger \hat{b}_0^\dagger \hat{b}_1 \hat{b}_{-1}), \end{aligned} \quad (\text{A5})$$

Compare to the only one spin-exchange process in single spinor BEC: ($a_0^\dagger a_0^\dagger a_1 a_{-1} + h.c.$), there are five heteronuclear spin-exchange processes inside the inter-species part

H_{12} ,

$$\begin{aligned}
H_{12} = & \beta(\hat{n}_1\hat{n}'_1 + \hat{n}_{-1}\hat{n}'_{-1} - \hat{n}_1\hat{n}'_{-1} - \hat{n}_{-1}\hat{n}'_1) \\
& + \gamma(\hat{n}_0\hat{n}'_0 + \hat{n}'_1 + \hat{n}_{-1}\hat{n}'_1) \\
& + \beta(\hat{a}_{-1}^\dagger\hat{a}_0\hat{b}_0^\dagger\hat{b}_{-1} + \hat{a}_0^\dagger\hat{a}_{-1}\hat{b}_{-1}^\dagger\hat{b}_0) \\
& + \beta(\hat{a}_1^\dagger\hat{a}_0\hat{b}_0^\dagger\hat{b}_1 + \hat{a}_0^\dagger\hat{a}_1\hat{b}_1^\dagger\hat{b}_0) \\
& + (\beta - \gamma)(\hat{a}_{-1}^\dagger\hat{a}_0\hat{b}_1^\dagger\hat{b}_0 + \hat{a}_0^\dagger\hat{a}_{-1}\hat{b}_0^\dagger\hat{b}_1) \\
& + (\beta - \gamma)(\hat{a}_1^\dagger\hat{a}_0\hat{b}_{-1}^\dagger\hat{b}_0 + \hat{a}_0^\dagger\hat{a}_1\hat{b}_0^\dagger\hat{b}_{-1}) \\
& + \gamma(\hat{a}_1^\dagger\hat{a}_{-1}\hat{b}_{-1}^\dagger\hat{b}_1 + \hat{a}_{-1}^\dagger\hat{a}_1\hat{b}_1^\dagger\hat{b}_{-1}), \quad (\text{A6})
\end{aligned}$$

We choose the following set of state vectors as the basis (or so called Schwinger presentation), where

$$\hat{L}_a^+ = \hat{a}_0^\dagger\hat{a}_{-1}, \hat{L}_a^- = \hat{a}_{-1}^\dagger\hat{a}_0, \hat{L}_a^z = \frac{1}{2}(\hat{n}_0 - \hat{n}_{-1}) \quad (\text{A7})$$

$$\hat{L}_b^+ = \hat{b}_1^\dagger\hat{b}_0, \hat{L}_b^- = \hat{b}_0^\dagger\hat{b}_1, \hat{L}_b^z = \frac{1}{2}(\hat{n}'_1 - \hat{n}'_0) \quad (\text{A8})$$

and we have,

$$\hat{L}_a^+ |m_1, m_2\rangle = j_a^+ |m_1 + 1, m_2\rangle, \quad (\text{A9})$$

$$\hat{L}_a^- |m_1, m_2\rangle = j_a^- |m_1 - 1, m_2\rangle, \quad (\text{A10})$$

$$\hat{L}_b^+ |m_1, m_2\rangle = j_b^+ |m_1, m_2 + 1\rangle, \quad (\text{A11})$$

$$\hat{L}_b^- |m_1, m_2\rangle = j_b^- |m_1, m_2 - 1\rangle, \quad (\text{A12})$$

$$\hat{L}_a^z |m_1, m_2\rangle = m_1 |m_1, m_2\rangle, \quad (\text{A13})$$

$$\hat{L}_b^z |m_1, m_2\rangle = m_2 |m_1, m_2\rangle \quad (\text{A14})$$

$$j_a^\pm = \sqrt{\left(\frac{N_a}{2} \pm m_1 + 1\right)\left(\frac{N_a}{2} \mp m_1\right)} \quad (\text{A15})$$

$$j_b^\pm = \sqrt{\left(\frac{N_b}{2} \pm m_2 + 1\right)\left(\frac{N_b}{2} \mp m_2\right)}. \quad (\text{A16})$$

Appendix B: The coherent state

In this section, we give a brief review of quantum ground states of spin-1 BEC. A scalar BEC consisting of N identical bosons can be described as a Fock state $|\Psi\rangle = (N!)^{-1/2}(\hat{a}^\dagger)^N |0\rangle$. If the internal degrees of freedom are considered, we can generalize a Fock state into a coherent state, if letting:

$$\hat{a}^\dagger \rightarrow \hat{\Gamma}_c^\dagger = \epsilon_1\hat{a}_1^\dagger + \epsilon_0\hat{a}_0^\dagger + \epsilon_{-1}\hat{a}_{-1}^\dagger, \quad (\text{B1})$$

with $\sum_{m=1,0,-1} |\epsilon_m|^2 = 1$. In the view of the single-particle concept, $\hat{\Gamma}_c^\dagger$ means creating one boson in an internal superposition state and the coefficients ϵ_m determine the orientation of the internal spin:

$$\begin{aligned}
\epsilon_1 &= \exp(-i\varphi) \cos^2\left(\frac{\theta}{2}\right), \\
\epsilon_0 &= \sqrt{2} \cos\frac{\theta}{2} \sin\frac{\theta}{2}, \\
\epsilon_{-1} &= \exp(-i\varphi) \sin^2\left(\frac{\theta}{2}\right). \quad (\text{B2})
\end{aligned}$$

As particles are not related to each other in the CSS, we can apply the direct product N times to get sufficient particle numbers. In the spin-1 system, the CSS is described as:

$$|\theta, \varphi\rangle = \frac{1}{\sqrt{N!}} (\hat{\Gamma}_c^\dagger)^N |0, 0, 0\rangle \quad (\text{B3})$$

with all the spins pointing into a definite direction. In particular, if we choose the total spin pointing to the positive direction of the x-axis ($\theta = \frac{\pi}{2}, \varphi = 0$), the CSS reads:

$$\left|\frac{\pi}{2}, 0\right\rangle = \frac{1}{\sqrt{N!}} \left(\frac{1}{2}\hat{a}_1^\dagger + \frac{1}{\sqrt{2}}\hat{a}_0^\dagger + \frac{1}{2}\hat{a}_{-1}^\dagger\right)^N |0, 0, 0\rangle \quad (\text{B4})$$

Similarly, the pseudospin-1/2 CSS is described as:

$$|\theta, \varphi\rangle^{(\frac{1}{2})} = \frac{1}{\sqrt{N!}} \left(\cos\left(\frac{\theta}{2}\right)\hat{a}_1^\dagger + e^{i\varphi} \sin\left(\frac{\theta}{2}\right)\hat{a}_2^\dagger\right)^N |0, 0\rangle. \quad (\text{B5})$$

Appendix C: Two-site Hubbard model

A brief review of quantum ground states of the two site Boson-Hubbard model is necessary. The Hamiltonian is

$$H = -t(a^\dagger b + b^\dagger a) + U[n_a(n_a - 1) + n_b(n_b - 1)] \quad (\text{C1})$$

with a and b denote the left and right site respectively. The hopping parameter is t and interaction is U . The Hilbert space is expanded by Fock state $|n_a, n_b\rangle$, or rewritten as $|m\rangle$:

$$|m\rangle = \frac{(\hat{a}^\dagger)^{\frac{N}{2}+m} (\hat{b}^\dagger)^{\frac{N}{2}-m}}{\sqrt{\left(\frac{N}{2} + m_1\right)!} \sqrt{\left(\frac{N}{2} - m_1\right)!}} |0\rangle. \quad (\text{C2})$$

Rewriting operators to be $a_\pm = (a^\dagger \pm b^\dagger)/\sqrt{2}$, the coherent ground state of Hubbard model is

$$\begin{aligned}
|G\rangle &= \frac{1}{\sqrt{N!}} (a_+^\dagger)^N |0\rangle = \frac{1}{\sqrt{2^N N!}} (a^\dagger + b^\dagger)^N |0\rangle \\
&= \sum_{m=-\frac{N}{2}}^{\frac{N}{2}} \frac{C_N^{\frac{N}{2}+m}}{\sqrt{2^N N!}} (a^\dagger)^{\frac{N}{2}+m} (b^\dagger)^{\frac{N}{2}-m} |0\rangle,
\end{aligned}$$

which has a gaussian amplitude distribution.